An NMR and Computational Study of a Lithium Amide and Ethereal Ligand Exchange

Göran Hilmersson*[a]

Abstract: The activation parameters for the exchange of an ethereal ligand in a chiral lithium amide was determined from full bandshape analysis of the dynamic NMR spectra. For diethyl ether, the activation parameters were $\Delta H^{\neq} = 11.0$ kcal mol^{-1} and $\Delta S^{\neq} = 12.0$ cal K^{-1} mol^{-1}. The exchange of the tetrahydrofuran ligand proceeds with a similar activation enthalpy $\Delta H^{\neq} = 11.2$ kcal mol^{-1}; however, the entropy is close to zero, $\Delta S^{\neq} = 1.6$ cal K^{-1} mol^{-1}. The dissociation of the ethereal ligand was also modeled by means of semiempirical (PM3) and density functional (DFT) methods. The experimental ^{13}C NMR chemical shifts for the carbons of uncoordinated and coordinated ethers were calculated with the GIAO-DFT (B3PW91/6-31G(d)) computational method.

Keywords: density functional calculations · ligand exchange · lithium · NMR spectroscopy

Introduction

Organolithium reagents constitute one of the most widely employed class of reagents in synthetic organic chemistry. Organolithium compounds are strong dipoles that aggregate to various extents in solution.[1] In coordinating solvents, such as ethers, these reagents are often dimeric or tetrameric. The use of Lewis bases is known to affect the reactivity and allows noncovalently bonded auxiliaries to be used for asymmetric reactions.[2] To be able to design such chiral additives, a detailed understanding of the thermodynamics and kinetics of ligand exchange is necessary. However, the details of this important process have not yet been investigated. For example, is the ligand exchange process driven by entropy or by enthalpy? A few years ago, some reports regarding slow ethereal ligand exchange rates appeared in the literature.[3] It was suggested that many lithiation reactions might proceed with the ethereal ligand exchange as the rate-limiting step.

Computational chemistry is now becoming an available technique for the evaluation of the structure of organic compounds. The semiempirical PM3 method, with Anders' parameters for lithium,[4] has been shown to adequately reproduce the geometries of organolithium compounds from experimental, density functional theory (DFT), and ab initio computational methods. However, the energies calculated with the PM3 method are usually poor.[5] Recently, Abbotto et al. showed that energies calculated with the density functional theory and a B3LYP hybrid functional with standard basis sets (6-31G(d) on the PM3-optimized geometries (B3LYP/6-31G(d)//PM3) reproduced higher level results (B3LYP/6-31G+(d)//B3LYP/6-31G+(d)) with high accuracy.[6]

Despite their high utility, computational studies of this type only provide information regarding the standard molar enthalpic contribution to the free energy, and should be thoughtfully interpreted since the entropy term is left out. This report demonstrates the fruitful combination of experimental and computational methods to yield detailed mechanistic information on the important ethereal ligand exchange. Furthermore, since ^{13}C chemical shifts provide a key to structure determination of organolithium compounds, we have explored the potential of theoretically calculated isotropic shielding constants as an additional source for the correct assignment of NMR signals.

The NMR calculation of the isotropic shielding constants of ^{13}C nuclei can provide additional support for structures, and also provide help in the choice between otherwise closely related structures. GIAO-DFT calculations of the isotropic shielding constants of the ^{13}C nuclei of various compounds have been reported. There are many accurate calculations of ^{13}C NMR chemical shifts.[7] The chemical shift calculations are sensitive and can provide an additional source for the correct assignment of NMR signals.

We have previously reported several studies on a chiral lithium amide, **Li-1**, and its solvates and mixed complexes with *n*BuLi by various NMR spectroscopic methods. This makes

[a] Prof. Dr. G. Hilmersson
Organic Chemistry, Department of Chemistry
Göteborg University
41296 Göteborg (Sweden)
Fax: (+46) 31-7723840
E-mail: hilmers@oc.chalmers.se

  0947-6539/00/0616-3069 $ 17.50+.50/0

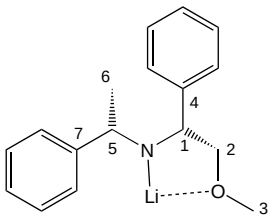

Li-1

this system particularly interesting since the structures and some of their dynamics are well understood. The dimer of **Li-1** only coordinates one ethereal ligand, even at higher concentrations of ether. Therefore, this is a key compound for studies of ligand exchange reactions. From the ^{13}C NMR experiments we have observed that the signals for the α-carbon atom of coordinated diethyl ether (DEE) in $(\mathbf{Li\text{-}1})_2 \cdot$DEE appear about 5 ppm upfield of the signal for uncoordinated DEE ($\delta = 60.6$ compared to 65.6 for free DEE).[3d,e] Interestingly, Lucht and Collum reported almost identical upfield shifts for the carbon atoms in the DEE solvate of lithium hexamethyldisilazide, LiHMDS, ($\delta = 60.4$) (Figure 1).[3a,b]

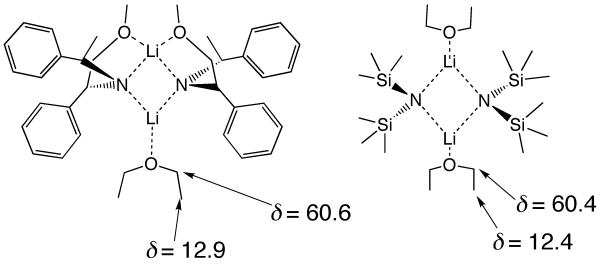

$(\mathbf{Li\text{-}1})_2$•DEE (LiHMDS)$_2$•2DEE

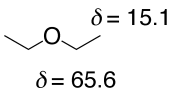

DEE

Figure 1. Structures and experimental ^{13}C NMR shifts of the α- and β-carbon atoms in the DEE solvates of $(\mathbf{Li\text{-}1})_2$ and lithium hexamethyldisilazide, as well as uncoordinated DEE.

In contrast, the α-carbon signals of tetrahydrofuran (THF) are shifted downfield by 0.7 ppm upon coordination to a lithium amide dimer. Again we reported almost identical shift changes for the α carbon of THF upon coordination to $(\mathbf{Li\text{-}1})_2$ to those reported by Lucht and Collum for the LiHMDS · THF solvate. Since **Li-1** and LiHMDS are structurally quite different lithium amides it is clear that the observed chemical shift changes result from the coordination of the lithium cation and not from specific interactions between the particular amide and the coordinating solvent. But what could be the reason for these changes in the chemical shifts? Clearly it could not be solely caused by coordination to the electron-poor lithium cation, since that is expected to result in decreased shielding and result in a downfield shift of the ether carbons. This is only observed for THF, but not for DEE. We have investigated these differences by means of a computational approach based on GIAO-DFT chemical shift anisotropic calculations.

Experimental Section

General: All glassware was dried overnight in a 120 °C oven (syringes were dried at 50 °C in a vacuum oven) before transfer into a glove box (Mecaplex GB 80 equipped with a gas purification system that removes oxygen and moisture) under an atmosphere of nitrogen. The typical moisture content was < 2 ppm. All manipulations of the lithium compounds were carried out in the glove box by means of gas-tight syringes. Ethereal solvents were stored and freshly distilled from Deporex (FLUKA AG) prior to use. The in-situ preparation of (2-methoxy-(*R*)-1-phenyl-ethyl)-(2-[^{6}Li]-lithium-(*S*)-1-phenylethyl)amide and characterization has been reported previously.[8]

NMR spectroscopy: All NMR spectra were recorded with a Varian Unity 500 spectrometer equipped with three channels and a 5 mm ^1H, ^{13}C, ^6Li triple-resonance probe head, built by the Nalorac company. Measuring frequencies were 500 MHz (^1H) and 125 MHz (^{13}C). The ^1H and ^{13}C spectra were referenced to the solvent [D_{10}]diethyl ether signals at $\delta = 1.06$ ($^1H{-}CH_3$) and $\delta = 15.2$ ($^{13}C{-}CH_3$), respectively. Probe temperatures were measured after more than 1 h of temperature equilibrium with both a calibrated methanol – Freon NMR thermometer and the standard methanol thermometer supplied by Varian instruments.[9]

Computational methods: Because of the considerable size of the aggregates under investigation, we restricted our geometry optimizations to semiempirical PM3 calculations.[4] The structures were reoptimized with the keyword HHon,[10] to eliminate the too positive HH attraction of the PM3 method. All geometries were characterized as either minimum or transition states by calculation of their frequencies at this level. Single-point calculations were performed at the B3LYP/6-31G(d) level of theory with the PM3-optimized structures. Geometry optimizations and frequency calculations were also performed for the DEE and THF structures at the B3LYP/6-31G(d) level of theory. The calculations were performed either with the Spartan program package[11] on a Silicon Graphics INDY workstation or with the Titan program package[12] on a PC (Pentium III, 600 MHz).

All the GIAO-DFT ^{13}C NMR chemical shift calculations were performed at the B3PW91/6-31G(d)[13] level of theory with the Gaussian 98[14] suite of programs on a Silicon Graphics Origin 200 computer.

Results and Discussion

Diethyl ether ethereal ligand exchange: The chiral lithium amide **Li-1** [0.70 M], was prepared in situ in [D_8]toluene. To the lithium amide was added one equivalent of diethyl ether (DEE), that is one DEE molecule per lithium amide molecule (Scheme 1). At -90 °C, the ^{13}C NMR spectra show a resonance at $\delta = 65.8$ for uncoordinated DEE and another at $\delta = 60.0$ for coordinated DEE. Therefore, the α-carbon atom of DEE is shifted upfield by 6 ppm upon coordination in $(\mathbf{Li\text{-}1})_2 \cdot$DEE (Figure 2a). Only signals from $(\mathbf{Li\text{-}1})_2 \cdot$DEE and free DEE are observed; no signals are observed for unsolvated $(\mathbf{Li\text{-}1})_2$ at any temperature. At very low [DEE]:[**Li-1**] ratios only $(\mathbf{Li\text{-}1})_2 \cdot$DEE is observed. Signals for free DEE,

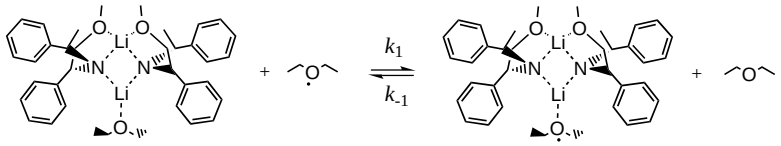

Scheme 1. Ligand exchange equilibrium of $(\mathbf{Li\text{-}1})_2 \cdot$DEE.

0947-6539/00/0616-3070 $ 17.50+.50/0 *Chem. Eur. J.* **2000**, *6*, No. 16

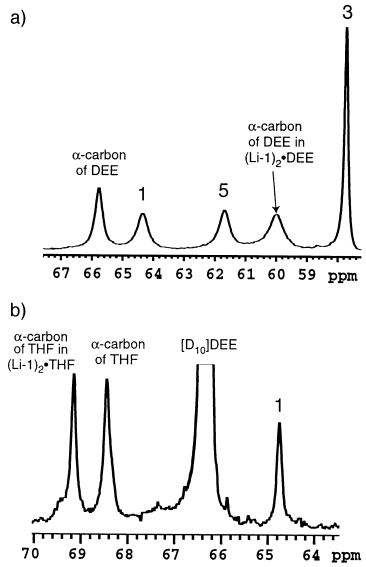

Figure 2. a) Selected region of the ^{13}C NMR spectrum (125 MHz) of $(\mathbf{Li\text{-}1})_2 \cdot$DEE [0.35 M] and DEE [0.35 M] in [D_8]toluene at $-90\,^{\circ}C$. b) Selected region of the ^{13}C NMR spectrum (125 MHz) of $(\mathbf{Li\text{-}1})_2 \cdot$THF [0.30 M] and THF [0.30 M] in [D_{10}]DEE at $-95\,^{\circ}C$.

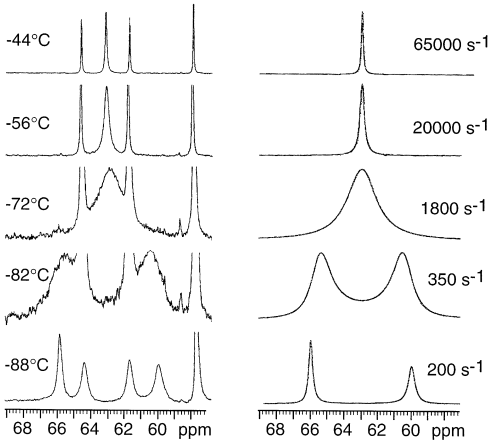

Figure 3. Experimental (left) and calculated (right) ^{13}C NMR spectra (125 MHz) of the α carbons of DEE. The differences in the temperature-dependent chemical shifts which were used in the calculation at fast exchange rates were extrapolated from the temperature dependence at slow exchange rates. Because of the difference in the relaxation times of free and complexed DEE at temperatures below $-80\,^{\circ}C$, these signals appear with different linewidths. This has been included in the calculations by the use of a slightly larger value for the linewidth of complexed DEE than for free DEE.

identical to those from pure DEE in toluene, are only observed for [DEE]:[**Li-1**] > 0.5. This indicates a very large equilibrium constant for the complexation of DEE by $(\mathbf{Li\text{-}1})_2$. At $-90\,^{\circ}C$, the DEE exchange rate is slow on the NMR timescale, whereas at higher temperatures the rate of exchange increases and the signals coalesce at $-71\,^{\circ}C$.[3d] At even higher temperatures, fast exchange yields the averaged signals for DEE (α- and β-carbon atoms).

An NMR tube with a 1:1 mixture of $(\mathbf{Li\text{-}1})_2 \cdot$DEE and DEE was prepared and a series of ^{13}C NMR spectra were obtained between -87 and $-29\,^{\circ}C$. The experiments were repeated with an independent sample with identical results.

The temperature-dependent NMR spectra were subjected to full bandshape analysis by means of the program gNMR.[15] The full bandshape analysis gives k_{obs} and the resulting calculated spectra for this degenerate two-site exchange. The observed ^{13}C NMR spectra are shown in Figure 3 along with the calculated spectra. The ligand exchange may, in principle, proceed with or without an intermediate, which could be either a disolvated or an unsolvated dimer. Our previous data indicates a dissociative mechanism. The rate-limiting step of such a two-step process must be the first step, the dissociation of the ether, since no intermediates are observed by NMR. The observed rate constant is the sum of the forward and the backward process according to Equation (1).

$$k_{obs} = 2k_1 \ (k_1 = k_{-1}) \quad (1)$$

The activation energies $\Delta G^{\neq}$ are calculated with the Eyring equation [Eq. (2)].

$$\Delta G^{\neq} = -RT\ln(k_1 h/k_B T) \text{ where } k_1 = k_{obs}/2 \quad (2)$$

The rate constants were determined at different temperatures and are given in Table 1. The Eyring plot (Figure 4) of the resulting kinetic data gives a straight line, and the activation parameters were interpolated: $\Delta G^{\neq}_{221\,K} = 8.3 \pm 0.2$ kcal mol^{-1}, $\Delta H^{\neq} = 11.0 \pm 0.3$ kcal mol^{-1} and $\Delta S^{\neq} = 12.0 \pm 6$ cal mol^{-1} K^{-1} ($T\Delta S^{\neq}_{221\,K} = 2.7$ kcal mol^{-1}), respectively.[16]

Table 1. Simulated rate constants for the exchange of diethyl ether with full lineshape analysis.

T[K]	Simulated rate constant[a] [s^{-1}]
244	250000
239	150000
234	105000
229	65000
223	36000
217	20000
212	8000
201	1800
196	750
191	350
185	200

[a] Full lineshape analyses were performed with the program gNMR, a product of CSC.[16] Estimated errors are less than $\pm 7\%$ based on full lineshape curve-fitting.

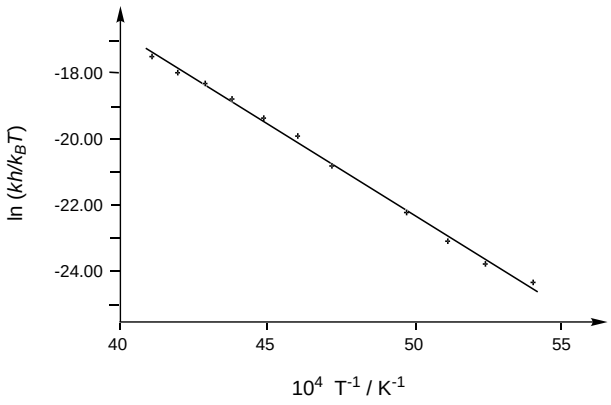

Figure 4. Eyring plot for the DEE ethereal ligand exchange between free DEE and coordinated DEE in $(\mathbf{Li\text{-}1})_2 \cdot$DEE in [$D_8$]toluene.

The entropy term is significantly smaller than the enthalpy term.

The positive entropy of activation supports the previous indication that the ligand exchange proceeds by a dissociative mechanism.[3d] In the transition state, the dissociating ethereal ligand gains some of its entropy which was lost upon coordination. The ether molecule enjoys less restricted motion by steric interaction in the transition state than in the initial state (coordinated). This could be the result of increased vibrational or internal rotational entropy.

THF ethereal ligand exchange: The chiral lithium amide **Li-1** [0.60 M] was also prepared in situ in [D_{10}]DEE. To the DEE solution of (**Li-1**)$_2$ · DEE was added one equivalent of THF, namely one THF molecule per lithium amide molecule. The ^{13}C NMR spectrum shows one set of signals for uncoordinated THF and another set for THF coordinated to (**Li-1**)$_2$, that is (**Li-1**)$_2$ · THF (Figure 2b). Thus slow ligand exchange is also observed for THF as with DEE. The ^{13}C NMR spectra shows a resonance at $\delta = 68.5$ for the free THF and another at $\delta = 69.2$ for the coordinated THF at $-95\,^{\circ}$C (Figure 2b). The signal of the α-carbon atom of THF is shifted downfield by 0.7 ppm upon coordination in (**Li-1**)$_2$ · THF. This is the opposite effect of that observed with DEE upon coordination to the same lithium amide dimer. Clearly, the equilibrium between DEE and THF solvated dimers strongly favors the THF solvate because no signals for (**Li-1**)$_2$ · DEE are observed.

Full bandshape analysis of the α-carbon signals was conducted on a series of ^{13}C NMR spectra of two samples collected at temperatures between -30 and $-77\,^{\circ}$C. The activation parameters, $\Delta G^{\neq}_{245\,K} = 10.9 \pm 0.2$ kcal mol^{-1}, $\Delta H^{\neq} = 11.2 \pm 0.3$ kcal mol^{-1}, and $\Delta S^{\neq} = 1.6 \pm 6$ cal mol^{-1} K^{-1} for the THF ethereal ligand exchange were obtained from the Eyring equation.[16] The activation enthalpy for THF ligand exchange was the same, within experimental errors, as that for DEE exchange, whereas the entropy of activation was significantly less for THF compared to that of DEE.

These results of the DEE and THF exchanges are interpreted in detail in the following section by means of computational methods.

Computational studies

The PM3 geometry-optimized structures of (Li-1)$_2$ · DEE and (Li-1)$_2$ · THF: The semiempirical PM3 method was employed to obtain the geometries of the structures of (**Li-1**)$_2$ · DEE and (**Li-1**)$_2$ · THF. The PM3 geometry-optimized structure of (**Li-1**)$_2$ · THF has already been discussed.[17] The distances between the lithium and the coordinating oxygen of the ethereal ligands were 2.06 Å (DEE) and 2.02 Å (THF). Single-point energy calculations of the relative solvation energies for the PM3-optimized geometries were performed at the B3LYP/6-31G(d) level of theory [Eq. (3)].

$$(\textbf{Li-1})_2 + S \rightleftharpoons (\textbf{Li-1})_2 \cdot S \qquad \Delta E_{solv} \tag{3}$$

Solvation energies for the equilibrium thus calculated give $\Delta E_{solv}(DEE) = -9.15$ kcal mol^{-1} and $\Delta E_{solv}(THF) = -10.94$ kcal mol^{-1} (Scheme 2).

Transition-state modeling of the ethereal ligand dissociation: The dissociation of DEE from (**Li-1**)$_2$ · DEE was modeled at the PM3 level. In the calculated structure of (**Li-1**)$_2$ · DEE, the Li–O_{DEE} distance is 2.05 Å. In the calculated transition state for the dissociation of the DEE from (**Li-1**)$_2$ the Li–O_{DEE} distance is 3.119 Å (Scheme 3). Single-point DFT energy calculations at B3PW91/6-31G(d)//PM3 and B3LYP/6-

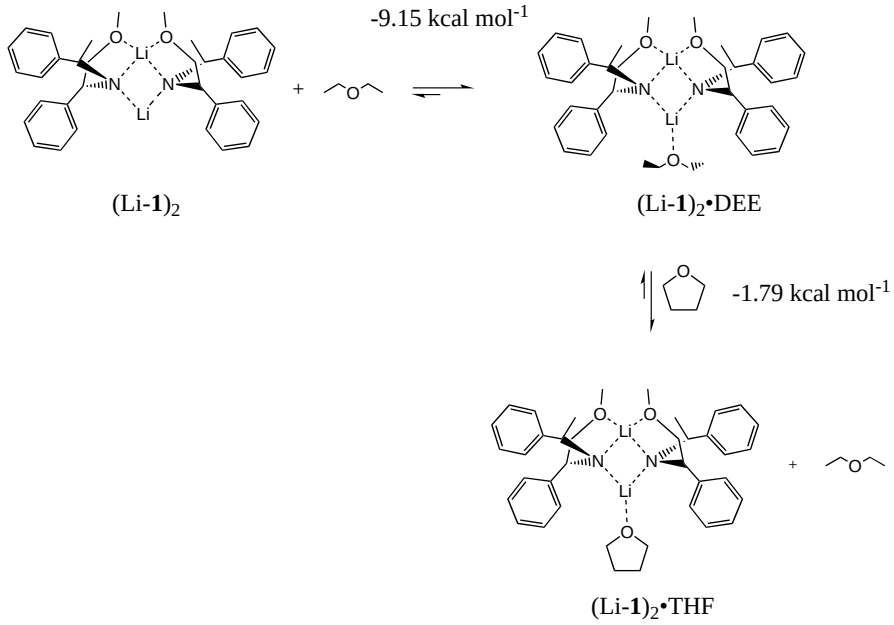

Scheme 2.

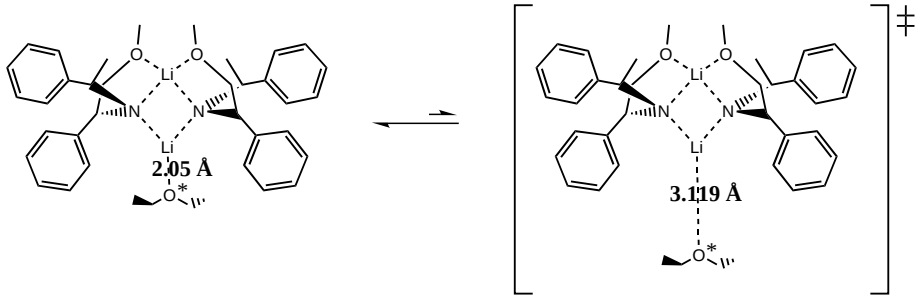

Scheme 3.

0947-6539/00/0616-3072 $ 17.50+.50/0 *Chem. Eur. J.* **2000**, *6*, No. 16

31G(d)//PM3 levels of theory gave activation energies of 7.2 and 7.3 kcal mol^{-1}, respectively. Considering the approximation introduced with the PM3 structures, these calculated activation energies are fairly close to the experimentally determined activation enthalpy of 11.0 kcal mol^{-1}.

Similarly, the activated complex for the THF dissociation transition state was found on the PM3 potential energy surface. Single-point DFT calculations were conducted to obtain the barrier for dissociation. From the B3LYP/6-31G(d)//PM3 calculations, we calculated the activation barrier for THF dissociation to be 9.5 kcal mol^{-1}. This value is close to the 11.2 kcal mol^{-1} obtained by full bandshape analysis of the dynamic NMR spectra.

Based on the results of the solvation energies and the activation energies, a standard free-enthalpy diagram can be constructed showing the relative energies. The standard enthalpic energy of uncoordinated (**Li-1**)$_2$ plus an ethereal ligand is too high (too little negative) compared to the solvate and transition states of, for example, (**Li-1**)$_2$·DEE and [(**Li-1**)$_2$--DEE]$^{\neq}$. This is compensated for by the entropy term, which is calculated to be $\approx$25 cal K^{-1} mol^{-1}, in agreement with other experimental data.[18]

Geometry optimizations of DEE and THF: There are several local energy minima or conformations for DEE (Scheme 4 and Table 2). The lowest DFT energy conformations at the

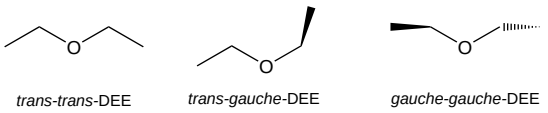

Scheme 4. Three conformations with local energy minima in the geometry optimization of DEE.

Table 2. Dihedral angles [°] and energies [Hartree] for the different DEE conformations. Energies in Hartrees and kcal mol^{-1} are also given for the different conformations of DEE obtained at the B3LYP/6-31G(d)//B3LYP/6-31G(d) level of theory.[a]

DEE conformer	ϕ_1	ϕ_2	E[Hartree]	Rel. energy [kcal mol^{-1}]
trans – trans	180.0	180.0	– 233.66341	0
trans – gauche	174.4	76.1	– 233.66127	1.34
gauch-gauche	60.0	60.0	– 233.65663	4.25
coordinated DEE (close to *gauche-gauche*)	65.0	65.2	–	–
DEE in the transition state	76.6	78.1	–	–

[a] The conformations of the coordinated DEE and the DEE in the transition state are those obtained from the PM3 calculations.

B3LYP/6-31(d)//B3LYP/6-31(d) level were calculated to be the planar *trans-trans* and the *trans-gauche* minima. The *trans-gauche* minimum is 1.34 kcal mol^{-1} higher in DFT energy than the planar *trans-trans* minimum. The estimated difference from IR studies is 1.4 kcal mol^{-1}.[19]

The conformation of the coordinated DEE is close to the *gauche-gauche* maximum. The two dihedral angles in the PM3-optimized geometry are 65.17 and 65.03°, respectively. This is fairly close to 60° which corresponds to a *gauche-gauche*-DEE. A DEE with a dihedral angle of 65° does not represent an energy minimum on the B3LYP/6-31G(d) potential energy surface. We can conclude that there is a substantial loss (more than 4 kcal mol^{-1}) of enthalpy because of the disfavored conformer that DEE must attain in order to coordinate to the lithium amide.

GIAO-DFT NMR chemical shift calculations: ***(Li-1)$_2$·DEE***: The isotropic shielding values were calculated with the GIAO method at the B3PW91/6-31G(d)//PM3 level of theory. The corresponding chemical shifts were calculated for the CH_2 carbon (C2) of **Li-1** in (**Li-1**)$_2$·DEE as the internal reference and its chemical shift was set to $\delta = 77.8$. There is a satisfying agreement between the experimental and the GIAO-DFT computational result (Table 3).

Table 3. Experimental (– 90 °C) and DFT-GIAO calculated ^{13}C NMR chemical shifts at B3PW91/6-31G(d)//PM3 level of theory for selected carbon atoms in (**Li-1**)$_2$·DEE and (**Li-1**)$_2$·THF with the C2 carbon of **Li-1** as the reference ($\delta = 77.8$ for (**Li-1**)$_2$·DEE and 78.4 for (**Li-1**)$_2$·THF).

	(**Li-1**)$_2$·DEE		(**Li-1**)$_2$·THF	
Carbon atom[a]	δ_{exp}	δ_{calc}	δ_{exp}	δ_{calc}
2 (internal reference)	77.8		78.4	
6	27.1	29.4	27.2	29.7
3	57.6	55.4	57.5	55.9
5	61.8	64.4	61.0	64.9
1	64.4	67.7	64.8	68.1
4	147.4	142.0	147.3	143.0
7	153.7	148.0	153.4	147.1
coordinated DEE (α-carbon)	60.0	60.5		
coordinated DEE (β-carbon)	11.9	13.1		
coordinated THF (α-carbon)			68.4	69.2
coordinated THF (β-carbon)			24.5	25.9

[a] The ^{13}C NMR signals of the aromatic carbon atoms have not been fully assigned and are therefore excluded.

The GIAO-DFT calculations of the shielding of the ^{13}C NMR shifts were performed with the B3PW91/6-31G(d) basis set on fully geometry-optimized DEE at B3LYP/6-31G(d). The calculated ^{13}C NMR chemical shifts of the α-carbon atom and the β-carbon atom of diethyl ether in its different conformations are given in Table 4. The calculated chemical shifts for the carbons of *trans-trans-DEE* are $\delta =$ 66.0 and 16.3, which are close to those obtained experimentally, namely $\delta = 65.8$ and 15.2. The shifts of DEE are rather sensitive to its conformation as deduced from the calculations.

Table 4. GIAO-DFT calculated chemical shifts[a] for DEE (B3PW91/6-31G(d)).

	δ_{exp} CH_3	δ_{exp} CH_2	δ_{calc} CH_3	δ_{calc} CH_2
DEE in {(**Li-1**)$_2$·DEE}[b]	11.9	60.0	13.1	60.5
Uncoordinated DEE (*trans – trans*)[c]	15.2	65.8	16.3	66.0
(*trans – gauche*)[c]			15.0[e]	63.5[e]
(*gauche – gauche*)[c]			14.3	60.2
DEE (extracted from (**Li-1**)$_2$·DEE)[d]			12.6	58.9

[a] C2 carbon atom of (**Li-1**)$_2$·DEE was used as the reference ($\delta = 77.8$). [b] The geometry of (**Li-1**)$_2$·DEE was optimized at the PM3 level. [c] The geometry of DEE was optimized at the B3LYP/6-31G(d) level. [d] Extracted from the PM3 geometry-optimized (**Li-1**)$_2$·DEE and used for the GIAO-DFT calculations as such. [e] The average of the shifts for the two magnetically nonequal set of carbon atoms.

The shifts for the carbons of DEE in the PM3-optimized structure of (**Li-1**)$_2$ · DEE were calculated to be $\delta = 60.5$ and 13.1. This should be compared to the experimental shifts of $\delta = 60.0$ and 11.9, respectively. Thus, there is a small (± 0.5 ppm) difference between the experimental and the calculated shifts for the α carbons of DEE (both free DEE and (**Li-1**)$_2$ · DEE).

The conformation of DEE complexed in (**Li-1**)$_2$ · DEE was used without geometry optimization to exclude the effects that proximate atoms in (**Li-1**) have on the ^{13}C NMR chemical shifts on coordinated DEE. The calculation of the chemical shifts on this conformer of DEE resulted in an even larger upfield shift of 5.7 ppm. Based on these calculations, we conclude that the large upfield chemical shift observed by NMR is mainly the result of conformational change of DEE upon coordination. The DEE becomes "locked" in a disfavored conformation, the carbon signals for such a conformation are calculated to be shifted largely upfield, $\Delta\delta = 7.1$, compared to that of *trans-trans* DEE. Thus if we only consider the effect of coordinating DEE to an electron-poor lithium cation and exclude any conformational changes, we obtain a calculated downfield shift of 1.6 ppm for the α-carbon atoms of DEE.

THF: THF molecules have much more restricted internal motions than does DEE because the oxygen and carbon atoms in THF are constrained in a five-membered ring with mainly ring-puckering.

Three different minima which result from ring puckering were found on the energy potential surface of THF at B3LYP/6-31G(d) level of theory (Scheme 5). The relative DFT energies are given in Table 5. The b-THF conformer is the most stable followed by the a-THF conformer.

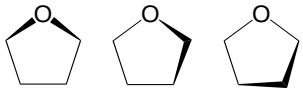

a-THF b-THF c-THF

Scheme 5. The three different minima which result from ring puckering that were found on the energy potential surface of THF at B3LYP/6-31G(d) level of theory.

Table 5. Calculated data for the THF conformers.

	Rel. energy [kcal mol^{-1}]	δ_{calc} α-carbon	δ_{calc} β-carbon
a-THF	0.0661	66.7	26.4
b-THF	0.0698	66.4	26.7
c-THF	0.0000	66.8	28.1

The GIAO-DFT ^{13}C NMR chemical shifts were also calculated for the conformers at the B3PW91/6-31G(d) level of theory. The THF ligand does not show the same large variation in ^{13}C NMR chemical shifts as did DEE.

*(**Li-1**)$_2$ · THF*: We also calculated the ^{13}C NMR isotropic shifts of (**Li-1**)$_2$ · THF and THF with GIAO-DFT at B3PW91/6-31G(d) level of theory. Again we used the CH_2 carbon atom of (**Li-1**)$_2$ · THF as the internal reference. The ^{13}C NMR chemical shifts for the carbons for (**Li-1**)$_2$ · THF are almost identical to those of (**Li-1**)$_2$ · DEE (Table 3).

However, here the effect of ethereal coordination to lithium is opposite to that on the chemical shifts for the carbon atoms of DEE. The α-carbon atoms of THF were calculated to shift ≈ 2 ppm downfield upon coordination. This must be caused by the coordination of the oxygen in THF, a Lewis base, to the electron-poor lithium cation. THF can not undergo a similar large conformational change as in DEE upon coordination. Hence only a small downfield shift is expected for THF upon coordination to (**Li-1**)$_2$ · THF. This is also observed experimentally with a 0.7 ppm downfield shift of the α-carbon atoms of THF upon coordination to (**Li-1**)$_2$ · THF.

Conclusions

The results of this study provide a possible explanation to why THF is a better ligand for lithium than DEE. The common belief has been that THF is a better ligand for cations because of its known larger dipole moment. We have shown that the enthalpic contributions to the ethereal ligand-exchange processes are equal for DEE and THF. However, the THF-solvated dimer is significantly more favored than that solvated by DEE.

There is a loss in enthalpy for DEE when it coordinates to lithium as it adopts a conformation which is higher in energy, although this loss in enthalpy is smaller than the solvation enthalpy. The difference in the ability of lithium to coordinate DEE and THF is, in part, caused by the greater loss in vibrational entropy (mainly internal rotational entropy) for DEE than THF. The vibrational entropy of DEE is calculated at B3LYP/6-31G(d) level of theory to be 6.7 cal mol^{-1} K^{-1} higher than in THF (ΔS_{vib}(DEE) = 15.1 cal mol^{-1} K^{-1} and ΔS_{vib}(THF) = 8.3 cal mol^{-1} K^{-1}).

The experimental results (the exchange rate is independent of the concentration with a positive entropy of activation) indicate a dissociative mechanism for the ethereal ligand exchange, a type of S_N1 reaction that proceeds through an intermediate unsolvated lithium amide dimer. The positive entropy term also indicates that there is an increased disorder in the transition state compared to the initial state. This is interpreted as a result of dissociation of a solvent molecule in the transition state.

The entropy associated with the dissociation of THF from its coordinated form to the transition state, [(**Li-1**)$_2$ $\cdots$ THF]‡ is significantly smaller compared to the entropy of activation observed with DEE. This difference is best explained if we compare the entropy loss upon coordination of the ethereal ligands to (**Li-1**)$_2$. Clearly, the coordination of DEE results in a substantial loss of vibrational and internal rotational entropy when the flexible DEE molecule becomes locked in a single conformation. In the case of THF, a much smaller loss of entropy is expected since THF is a five-membered cyclic compound with mainly ring-puckering vibrations. Some of this entropy will be released on transformation from the coordinating initial state to the transition state. The entropy of activation is thus larger for the DEE than for THF.

0947-6539/00/0616-3074 $ 17.50+.50/0 *Chem. Eur. J.* **2000**, *6*, No. 16

A possible associative mechanism (an S_N1 type with an intermediate disolvated lithium amide dimer) was also investigated; however, the energy for such an intermediate was found to be less favorable than that of the dissociative mechanism. Furthermore, an interchange mechanism of an S_N2-type reaction results in much higher activation energy. The possibility of an associative mechanism was not considered further.

The GIAO-DFT calculations have also been used to rationalize the large upfield shift observed for the α-carbon atoms of DEE upon coordination to be largely associated with a conformational change rather than coordination to a cation.

Furthermore, GIAO-DFT chemical shift calculations at the B3LYP level on the PM3 geometry-optimized structures reproduces the experimentally observed shifts very well. The largest differences between experimental and calculated shifts were ± 2 ppm. We may, therefore, propose that the GIAO-DFT method could become invaluable as an independent parameter for resonance assignments for complicated structures and aggregates that involve organolithium compounds.

Acknowledgements

Prof. Per Ahlberg and Dr. Per I. Arvidsson are gratefully acknowledged for their valuable suggestions of improvements on this manuscript. The author is grateful to Docent Ö. Davidsson for the synthesis of amine **1**. Financial support from the Swedish Natural Science Research Council and the Carl Trygger Foundation is also acknowleged.

[1] a) W. Bauer, P. von R. Schleyer in *Advances in Carbanion Chemistry*, *Vol. 1* (Ed.: V. Snieckus), JAI Press, Greenwich (Connecticut), **1992**, pp. 89–175; b) H. Günther, *Advanced Application of NMR to Organometallic Chemistry,* in *Physical Organometallic Chemistry, Vol. 1* (Eds.: M. Gielen, R. Willem, B. Wrackmeyer), Wiley, Chichester **1996**, p. 247–290.

[2] a) M. B. Eleveld, H. Hogeveen, *Tetrahedron Lett.* **1984**, *25*, 5187; b) T. Mukaiyama, K. Soai, T. Sato, H. Shimizu, K. Suzuki, *J. Am. Chem. Soc.* **1979**, *101*, 1455; c) L. Colombo, C. Gennari, G. Poli, C. Scolastico, *Tetrahedron* **1982**, *38*, 2725; d) D. Seebach, H.-O. Kalinowski, B. Bastani, G. Crass, H. Daum, H. Dörr, N. P. DuPreez, V. Ehrig, W. Langer, C. Nüssler, H.-A. Oei, M. Schmidt, *Helv. Chim. Acta* **1977**, *60*, 301; e) J.-P. Mazaleyrat, D. J. Cram, *J. Am. Chem. Soc.* **1981**, *103*, 4585.

[3] a) B. L. Lucht, D. B. Collum, *J. Am. Chem. Soc.* **1994**, *116*, 6009; b) D. B. Collum, B. L. Lucht, *J. Am. Chem. Soc.* **1995**, *117*, 9863; c) H. J. Reich, K. J. Kulicke, *J. Am. Chem. Soc.* **1996**, *118*, 273; d) G. Hilmersson, Ö. Davidsson, *J. Org. Chem.* **1995**, *60*, 7660–7669; e) G. Hilmersson, P. Ahlberg, Ö. Davidsson, *J. Am. Chem. Soc.* **1996**, *116*, 3539.

[4] a) J. J. P. Stewart, *J. Comput. Chem.* **1989**, *10*, 209; b) E. Anders, R. Koch, P. Freunscht, *J. Comput. Chem.* **1993**, *14*, 1301–1312.

[5] a) H. Weiss, A. V. Yakimansky, A. H. E. Müller, *J. Am. Chem. Soc.* **1996**, *118*, 8897–8903; b) P. I. Arvidsson, G. Hilmersson, P. Ahlberg, *J. Am. Chem. Soc.* **1999**, *121*, 1883–1887.

[6] A. Abbotto, A. Streitwieser, P. v. R. Schleyer, *J. Am. Chem. Soc.* **1997**, *119*, 11255–11268.

[7] a) J. R. Cheeseman, G. W. Trucks, T. A. Keith, M. J. Frisch, *J. Phys. Chem.* **1996**, *104*, 5497; b) W. B. Smith, *Magn. Reson. Chem*. **1999**, *37*, 103–106.

[8] G. Hilmersson, Ö. Davidsson, *J. Orgmet. Chem.* **1995**, *489*, 175–179.

[9] C. Engdahl, P. Ahlberg, *J. Am. Chem. Soc.* **1979**, *101*, 3940.

[10] G. I. Csonka, *J. Comput. Chem.* **1993**, *14*, 895—898;S. O. Nilsson Lill, P. Arvidsson, P. Ahlberg, *Tetrahedron Asymmetry* **1999**, 265–279.

[11] SPARTAN Version 5.0.1, **1995**, Wavefunction, Inc., 18401 Von Karman Ave., #370 Irvine, CA 92715 (USA).

[12] Titan Version 1.0.1, **1995**, Wavefunction, Inc., 18401 Von Karman Ave., #370 Irvine, CA 92715 (USA), and Schrödinger, Inc., 1500 SW First Avenue, #1180 Portland, OR 97201 (USA).

[13] J. P. Perdew; Y. Wang, *Phys. Rev. B* **1992**, *45*, 13244.

[14] Gaussian 98: M. J. Frisch, G. W. Trucks, H. B. Schlegel, G. E. Scuseria, M. A. Robb, J. R. Cheeseman, V. G. Zakrzewski, Montgomery, J. A., R. E. Stratmann, J. C. Burant, S. Dapprich, J. M. Millam, A. D. Daniels, K. N. Kudin, M. C. Strain, O. Farkas, J. Tomasi, V. Barone, M. Cossi, R. Cammi, B. Mennucci, C. Pomelli, C. Adamo, S. Clifford, J. Ochterski, G. A. Petersson, P. Y. Ayala, Q. Cui, K. Morokuma, D. K. Malick, A. D. Rabuck, K. Raghavachari, J. B. Foresman, J. Cioslowski, J. V. Ortiz, B. B. Stefanov, G. Liu, A. Liashenko, P. Piskorz, I. Komaromi, R. Gomperts, R. L. Martin, D. J. Fox, T. Keith, M. A. Al-Laham, C. Y. Peng, A. Nanayakkara, C. Gonzalez, M. Challacombe, P. M. W. Gill, B. Johnson, W. Chen, M. W. Wong, J. L. Andres, C. Gonzalez, M. Head-Gordon, E. S. Replogle, J. A. Pople, Gaussian Inc., Pittsburg, PA, **1998**.

[15] gNMR Version 4.1, Cherwell Scientific Limited, The Magdalen Centre Oxford Science Park, Oxford OX3 4GA (UK). This software calculates the full bandshape of signals that are broadened as a result of chemical exchange. The method is based on that of Binsch, see G. Binsch, *J. Am. Chem. Soc*. **1969**, *91*, 1304; D. S. Stephenson; G. Binsch, *J. Magn. Res.* **1978**, *30*, 625.

[16] The reported errors are the maximum errors obtained from a propagation calculation based on a maximum error of 7% in the rate constants and one degree of temperature error.

[17] G. Hilmersson, P. I. Arvidsson, Ö. Davidsson, *J. Am. Chem. Soc.* **1998**, *120*, 8143–8149.

[18] P. Ahlberg, A. Karlsson, Ö. Davidsson, G. Hilmersson, M. Löwendahl, *J. Am. Chem. Soc.* **1997**, *119*, 1751–1757.

[19] W. L. Jorgensen, M. Ibrahim, *J. Am. Chem. Soc.* **1981**, *103*, 3976–3985.

Received: December 27, 1999 [F2210]